Article

Journal of the Brazilian Chemical Society

https://dx.doi.org/10.21577/0103-5053.20240136

J. Braz. Chem. Soc. **2024**, *35*, 10, e-20240136, 1-9

Interaction of a Triruthenium *ortho*-Metallated Phenazine with Cytochrome P450 Enzymes

Luis Guilherme A. do Nascimento, [a] ***Maike F. S. Barbetta,*** [b] ***Otávio A. Chaves,*** [c,d] ***Anderson R. M. de Oliveira*** [*,b] ***and Sofia Nikolaou*** [*,a]

[a]*Laboratório de Atividade Biológica e Química Supramolecular de Compostos de Coordenação (LABiQSC²), Departamento de Química, Faculdade de Filosofia, Ciências e Letras de Ribeirão Preto, Universidade de São Paulo, Av. Bandeirantes, 3900, 14040-901 Ribeirão Preto-SP, Brazil*

[b]*Laboratório de Metabolismo in vitro e Técnicas de Separação, Departamento de Química, Faculdade de Filosofia, Ciências e Letras de Ribeirão Preto, Universidade de São Paulo, Av. Bandeirantes, 3900, 14040-901 Ribeirão Preto-SP, Brazil*

[c]*CQC-IMS, Departamento de Química, Universidade de Coimbra, Rua Larga, 3004-535 Coimbra, Portugal*

[d]*Laboratório de Imunofarmacologia, Centro de Pesquisa, Inovação e Vigilância em COVID-19 e Emergências Sanitárias (CPIV), Instituto Oswaldo Cruz (IOC), Fundação Oswaldo Cruz (Fiocruz), Av. Brasil, 4036, Bloco 2, 21040-361 Rio de Janeiro-RJ, Brazil*

The triruthenium *ortho*-metallated phenazine $[Ru_3O(CH_3COO)_5(py)_2(dppzCl)]PF_6$ (**1**, py = pyridine; dppz-Cl = 7-chlorodipyrido[3,2-*a*:2',3'-*c*]phenazine) is a potential metallo-drug candidate with *in vitro* anticancer and trypanosomicidal activities. It also showed strong interactions with deoxyribonucleic acid (DNA) and human serum albumin due to the presence of the planar and π-conjugated phenazine in its structure. Pursuing our interest in compound **1** behavior in a biological environment, we described its interaction with the cytochrome P450 (CYP450) enzymes present in human liver microsomes through a preliminary *in vitro* metabolism assay. This study showed that the human liver microsomes metabolized compound **1** in a concentration dependent manner. A phenotyping study suggests that CYP3A is the primary enzyme involved in the interaction, even though other isoforms metabolized **1** in a minor extent. It is worth mentioning that the results of phenotyping using supersomes should be interpreted cautiously, taking into account the inhibitory effect of the surfactant employed. Blind molecular docking results agreed with the experimental trend, showing the highest interactive profile with the isoforms CYP3A4 and 3A5, and suggested hydrophobic, π-stacking, and hydrogen bonds as the primary intermolecular forces responsible for the protein-compound interaction.

Keywords: triruthenium *ortho*-metallated phenazine, metallo-drug, cytochrome P450, *in vitro* metabolism, phenotyping, blind molecular docking

Introduction

Phenazines are organic molecules bearing fused aromatic rings with electron-deficient π-system and lone electron pairs on *N*-heteroatoms. Their core is a central 1,4-diazabenzene moiety with two annulated benzene rings. There is a large variety of derivatives from this basic structure, both natural and synthetic, being the reaction of benzoquinones and *o*-phenylenediamines the more straightforward way to obtain them.[1,2] The interest in these molecules arises from their wide range of biological activities, such as antimicrobial, antiparasitic, antitumor, anti-inflammatory, and neuroprotective.[3-6] Phenazines may also be combined with units such as two pyridines, generating, among other options, a phenanthroline framework, yielding a coordination bidentated ligand such as the dipyridophenazine (dppz, dipyrido[3,2-*a*:2',3'-*c*] phenazine). In these cases, the main interest relies on the ability of dppz to intercalate into the deoxyribonucleic acid (DNA) strands, interfering with its functions.[7]

*e-mail: sofia@ffclrp.usp.br

Editor handled this article: Carlos Maurício R. de Sant'Anna (Guest)

With this publication, the authors would like to honour Prof Eliezer J. Barreiro who, like many of us, has dedicated his life to increasing Brazilian knowledge about new drug candidates.

On the other hand, metallo-drugs are molecules with one or more transition metal ions in their structure and have potential biological activity.[8] In particular, ruthenium compounds are excellent candidates for developing new drugs, owing to their anticancer ability, mainly in the metastasis phase,[9,10] among other actions.[11,12] Such characteristics boosted the investigation of these molecules from the perspective of their biological applications.[13,14] An interesting class of ruthenium compounds is the trinuclear acetates with μ_3-oxo bridge[15,16] since these molecules display promising biological roles as probed by *in vitro* studies of their anticancer,[17-19] trypanosomicidal[19,20] or vasorelaxant activities.[21,22] Despite these properties, studies of these carboxylates are still scarce when compared with mononuclear molecules. Therefore, we highlight here the asymmetric compound $[Ru_3O(CH_3COO)_5(py)_2(dppzCl)]PF_6$ (**1**, py = pyridine; dppzCl = 7-chlorodipyrido [3,2-*a*:2',3'-*c*]phenazine, Figure 1). Within five *ortho*-metallated phenazines, the chloro-substituted dppz complex decreases murine melanoma cancer cell viability (B16F10 line) by more than 60% at 2 μmol L^{-1}, with little effect on the healthy cells (L929 fibroblast). It also presented a low half maximal inhibitory concentration (IC_{50}) value (0.21 μmol L^{-1}) toward the amastigote form of the *Trypanosoma cruzi* parasite, found in the chronic phase of Chagas disease.[19] The compound utilizes the dppzCl *ortho*-metallation reaction to insert a hydrophobic/intercalation site in the triruthenium structure for biotarget interactions.[23,24]

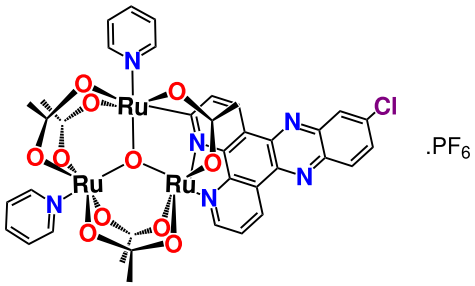

Figure 1. Structure of $[Ru_3O(CH_3COO)_5(py)_2(dppzCl)]PF_6$.

Because the $[Ru_3O(CH_3COO)_5(py)_2(dppzCl)]PF_6$ compound has shown promising biological activities *in vitro*, its ability to interact with relevant targets such as DNA and human serum albumin (HSA) was characterized as well.[19] As expected, the *ortho*-metallated dppzCl assisted the intercalation of compound $[Ru_3O(CH_3COO)_5(py)_2(dppzCl)]PF_6$ into the DNA strands, although its intercalation seemed not to be responsible for the observed anticancer activity. More interestingly, this compound strongly interacted with HSA, significantly changing its secondary structure.

In the present work, we aimed to expand our knowledge on the interactions of compound **1** with relevant proteins, addressing its interaction with the human cytochrome P450 (CYP450) enzymes through a preliminary *in vitro* metabolism assay. A phenotyping study was also undertaken to suggest with which isoform it interacts preferentially. In addition, blind molecular docking calculations revealed which intermolecular forces are responsible for these interactions.

Experimental

The complex $[Ru_3O(CH_3COO)_5(py)_2(dppzCl)]PF_6$ employed here was synthesized and characterized elsewhere.[25] The UV-Vis absorption and ^1H nuclear magnetic resonance (NMR) data and spectra (Figures S1 and S2, respectively) are available in the Supplementary Information (SI) section. The preliminary *in vitro* metabolism study and the enzyme phenotyping were checked by high-performance liquid chromatography (HPLC) after incubation of compound **1** with human liver microsomes (HLM) and recombinant CYP450 forms (rCYP450), respectively. Before the *in vitro* metabolism study, the bioanalytical method was fully validated according to the Agência Nacional de Vigilância Sanitária (ANVISA) guideline.[26] Details on part of the procedures and results, such as method validation, chromatographic analysis, *in vitro* metabolism, are also available in the SI section.

Solution preparation

The following stock solutions were prepared in their respective solvents and stored at −20.0 ºC: $[Ru_3O(CH_3COO)_5(py)_2(dppzCl)]PF_6$ at the concentrations of 600, 100, 80.0, and 50.0 μmol L^{-1} in acetonitrile; propranolol, used as internal standard (IS), in acetonitrile at the concentration of 100 μmol L^{-1} acquired from Sigma-Aldrich (St. Louis, USA). The solutions for the NADPH regeneration system (β-nicotinamide adenine dinucleotide phosphate hydrate) at the concentration of 2.50 mmol L^{-1}; glucose-6-phosphate sodium salt at the concentration of 50.0 mmol L^{-1}; and glucose-6-phosphate dehydrogenase at the concentration of 8.0 U mL^{-1} were prepared in tris-KCl buffer (tris(hydroxymethyl)aminomethane 0.05 mol L^{-1} and KCl 0.15 mol L^{-1}, pH 7.4) and also purchased from Sigma-Aldrich (St. Louis, USA). HLM (poll of 150 donor, mixed gender, 20 mg mL^{-1} microsomal protein) and rCYP450 (Supersomes®) were purchased from Corning Life Science (Phoenix, AZ, USA) and stored at −80.0 °C. Information about the products are presented in the SI section (Table S9).

All the solvents and reagents were HPLC and analytical grade, respectively. Methanol and acetonitrile were purchased from Êxodo Científica (Sumaré, Brazil), chloroform and formic acid were purchased from Sigma-Aldrich (St. Louis, USA), and Tween 80® was purchased from Dinâmica (Indaiatuba, SP, Brazil).

HPLC analysis

The analysis was carried out in a Shimadzu HPLC system (Kyoto, Japan), which comprised a DGU-20A5 online degasser, two LC-10AD solvent pump units, a SIL-20AHT automatic injector, a CTO-10AVP column oven, a SPD-M20A diode array detector, and a CBM-20A system controller. The analytical column used was a LiChroCART Si 60 (125 mm × 4 mm; 5 µm), and methanol:acetonitrile (80:20, v/v + 0.1% formic acid) was used as mobile phase at a flow rate of 0.6 mL min^{-1}. The injection volume was 10 µL and the oven temperature was 30 °C. The detection was performed at 280 nm (for IS), 350 nm and 680 nm (for the complex).

Sample preparation procedure

The microsomal samples (0.1 mol L^{-1} phosphate buffer, pH 7.4 with 0.2% of Tween 80®, HLM with 0.2 mg mL^{-1} of microsomal protein and NADPH cofactor) were extracted with 1000 µL of chloroform. To accomplish that, the samples were agitated for 15 min at 1000 rpm in Vibrax VXR® agitator (IKA, Staufen, Germany) at room temperature. After that, the samples were centrifuged at 1600 × *g* for 10 min at 4.0 °C in a Hitachi HIMAC CF 15D2 centrifuge (Hitachi, Tokyo, Japan). Next, 900 µL of the organic phase was collected and evaporated in a Concentrator Plus speed vacuum (Eppendorf, Hamburg, Germany). The sample residue was resuspended in the mobile phase and analyzed by HPLC according to the method described in HPLC analysis section.

In vitro metabolism and enzyme phenotyping

The incubation conditions for the *in vitro* metabolism with HLM was based on the procedure reported by Costa *et al*.[27] The incubation medium consisted of 5.0 µL of $[Ru_3O(CH_3COO)_5(py)_2(dppzCl)]PF_6$ (1.25, 2.00 or 2.50 µmol L^{-1}), 95.0 µL of phosphate buffer (0.1 mol L^{-1}, pH 7.4) with 0.2% of Tween 80®, and 50.0 µL of HLM (0.2 mg mL^{-1} of microsomal protein). The pre-incubation was performed for 5 min in a thermostatic water bath at 37.0 ºC. The metabolic reaction was started by the addition of 50.0 µL of the NADPH cofactor solution. After 40 min of incubation, the reaction was ended by the addition of chloroform and beginning of the sample preparation procedure. The samples were analyzed by the validated HPLC method, and the remaining percentage of the complex was determined considering a control sample prepared in the absence of NADPH cofactor solution. The difference between the initial and remaining complex concentration was considered CYP450 mediated metabolism.

To evaluate the main CYP450 isoform(s) that is (are) involved in the complex metabolism, rCYP450 was used. To accomplish that, $[Ru_3O(CH_3COO)_5(py)_2(dppzCl)]PF_6$ complex (1.25 µmol L^{-1}) was incubated, in a similar way to the previous procedure, with the following Supersomes®: 1A2; 1A1; 2B6; 2C8; 2C9; 2C19; 2D6; 2E1; 3A4; and 3A5 at the concentration of 50.0 pmol mL^{-1}. The control samples contained insect cells instead of rCYP450. The samples were quantified using an analytical curve prepared on the day of the experiment and the normalized depletion velocity of compound **1** was calculated for each rCYP450. In addition, for the statistical treatment, the normalized rate (NR) (equation 1) was determined using the abundance of each isoform in the human liver microsomes ($[CYP]_{HLM}$).[28]

$$NR = v_0 \times [CYP]_{HLM} \quad (1)$$

where v_0 is the initial velocity of the enzyme reaction. In this way, the total normalized rate (TNR) can be calculated by dividing NR by the sum of all NR considered (equation 2).

$$TNR\ (\%) = \frac{NR}{\sum NR} \times 100 \quad (2)$$

To evaluate the inhibitory effect of Tween 80® on rCYP450, the incubation media were prepared following the method outlined in the phenotyping studies, with compound **1** replaced by a probe substrate specific to each CYP450 isoform near its concentration to achieve half of the maximum velocity, the Michaelis-Menten constant (K_M) value. Inhibition controls for the probe substrates involved substituting the volume of phosphate buffer with Tween 80® with a pure buffer solution. Subsequent analysis of the samples yielded the remaining activity (RA / %), calculated by dividing the area of the monitored metabolite (probe marker) in the presence of Tween 80® by the area of the metabolite in its absence, and multiplying the result by 100%. Further details on the incubation procedure and HPLC analysis can be found in the SI section.

Molecular docking procedures

The crystallographic structures for 1A1, 1A2, 2C8,

2C9, 2C19, 2D6, 2E1, 3A4, and 3A5 were obtained from Protein Data Bank (PDB)[29] with access code 4I8V, 2HI4, 1PQ2, 1R9O, 4GQS, 4WNV, 3E6I, 1W0F, and 7LAD, respectively.[30-38] All hydration molecules and the small organic/inorganic charged species were deleted before *in silico* calculations. The chemical structure for the compound $[Ru_3O(CH_3COO)_5(py)_2(dppzCl)]PF_6$ was built, and the energy was minimized with semi-empirical method, available in the Spartan'18 software.[39,40] The blind molecular docking calculations in vacuum were performed with GOLD 2022.3 software.[41,42] Hydrogen atoms were added to the proteins following tautomeric states and ionization data inferred by GOLD 2022.3 software at pH 7.4. Each docking run's number of genetic operations (crossover, migration, mutation) was set to 100,000. Each CYP450 isoform obtained ten results and analyzed those with the highest docking score value. GOLD 2022.3 software optimizes hydrogen-bond geometries by rotating hydroxyl and amino groups of amino acid side chains. Since there is not any crystallographic data with CYP450 isoform complexed with inorganic species similar to compound **1** redocking studies were not carried out and for this reason, the standard ChemPLP was used as the scoring function. Protein-Ligand Interaction Profiler (PLIP) webserver[43,44] was used for the identification of protein-ligand interactions and the 3D-figures were generated by PyMOL Molecular Graphics System 1.0 level software.[45,46]

Results and Discussion

Redox mediators, such as ascorbic acid or cytochrome oxidase, may access the ruthenium oxidation states II, III, and IV in the physiological environment.[47] In these oxidation states, ruthenium ions are mainly hexacoordinated with pseudo-octahedral geometry, and Ru^{III}-compounds are relatively inert compared to cisplatin (*cis*-$[Pt(NH_3)_2Cl_2]$).[47,48] Redox biotransformation processes can either activate or transform a given molecule, changing properties such as hydrophilicity and thus affecting processes such as excretion.[49] CYP450 enzymes are predominant in the liver,[49] and it is the main enzyme family involved in xenobiotics redox biotransformation.[27] Investigating the interaction of a potential drug candidate with these enzymes and determining which CYP isoform interacts preferentially (enzyme phenotyping) is a key step to evaluate its metabolization profile and address its biological behavior and safety.[50-52]

In biotransformation studies with microsomes, the *in vitro* metabolism can be carried out by monitoring either substrate depletion or metabolite production. Since compound **1** is a novel molecule and information about possible metabolites is absent, the *in vitro* metabolism was carried out by monitoring the depletion of **1** after incubation with HLM. In addition, to guarantee the solubility of **1** in the microsomal medium, a solubilizing agent was used (0.2% Tween 80®). Since quantifying the depletion of the complex from the microsomal medium necessitated its complete solubilization, this was successfully achieved solely through the use of the surfactant Tween 80®.[53] Figure 2a shows a representative pair of chromatograms obtained in the analysis. As depicted in Figure 2b, at a concentration of 2.50 μmol L^{-1}, compound **1** exhibited a low metabolic rate, suggesting that the reaction had achieved its maximum velocity. This observation may be attributed to an inhibitory effect on the CYP450 enzymes induced by the presence of the solubilizing agent (Tween 80®), or potentially by the complex itself at this concentration.[54] Conversely, upon reducing the concentration of compound **1** to 1.25 μmol L^{-1}, the metabolic rate increased to 48%, indicating the capability of human CYP450 enzymes to metabolize the complex. Lower concentrations appear to facilitate its metabolism, notwithstanding potential inhibition by Tween 80® at the employed concentration. No discernible peaks of potential metabolites were observed during the metabolism studies. This absence could be attributed to factors such as the low concentration in the final solution, the limited extraction rate during sample preparation, diminished intensity due to peak broadening after extended retention times, or a combination thereof. Regarding the phenotyping study, all the investigated rCYP450 isoforms contributed to compound **1** metabolization, with significant contributions of CYP3A4 and CYP3A5 isoforms as it can be observed in the TNR percentage (Figure 2c). This result agrees with the literature[55,56] since these isoforms typically metabolize substrates with high molecular weight and low water solubility as compound **1**.

It is worth mentioning that the inclusion of Tween 80® in the phenotyping studies resulted in an inhibitory effect of varying degrees depending on the isoform, as indicated by the inhibition evaluation using probe substrates (Table 1); therefore, results of phenotyping using supersomes should be interpreted cautiously. The isoforms most affected were CYP1A1, CYP2B6, CYP2E1, and CYP3A4, with remaining activities (RA) ranging between 18-24%. Conversely, minimal to negligible effects were observed for CYP1A2, CYP2C9, CYP2D6, and CYP3A5, with RAs exceeding 90%. The inhibition of a specific isoform does not necessarily indicate an increased involvement in the metabolic reaction but rather implies a potential underestimation of its role, which remains unclear under the experimental conditions. It is worth noting that, apart from CYP2C19 and CYP3A4, the most abundant isoforms in humans were not significantly

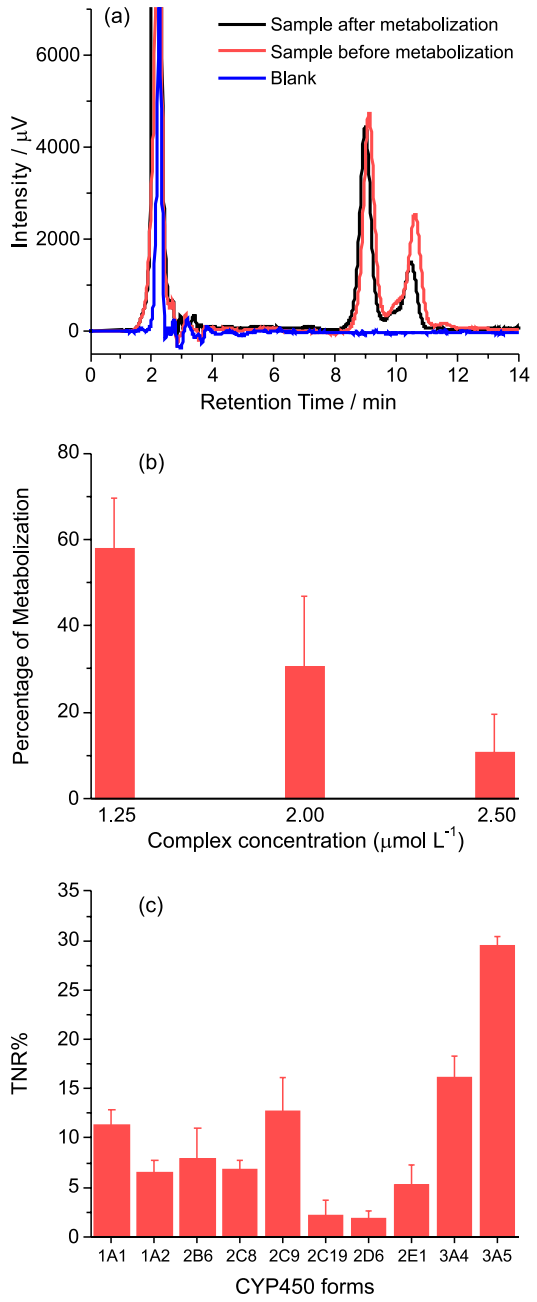

Figure 2. (a) Example of $[Ru_3O(CH_3COO)_5(py)_2(dppzCl)]PF_6$ (1.25 µmol L^{-1}) chromatograms before and after *in vitro* metabolism by the human CYP450 enzymes. (b) *in vitro* metabolism by the CYP450 enzymes present in human liver microsomes after incubation with different complex concentrations. (c) Total normalized rate of metabolization by the main rCYP450 isoforms responsible for human metabolism. n = 5 experiments *per* determination. In all cases, the control sample were prepared in the absence of NADPH cofactor.

inhibited (RA > 90%), and CYP3A5, which contributed significantly to the metabolism of compound **1**, remained uninhibited. Moreover, despite reduced activity, CYP3A4 still played a substantial role in the metabolism of **1**.

In silico calculations using a blind molecular docking approach were carried out to offer a molecular point of view on the interaction between compound **1** and the different CYP450 isoforms. Since each pose obtained by GOLD 2022.3 software is considered the negative value of the energy terms sum from the mechanical-molecular type component, a more positive docking score indicates better interaction. The docking score value for the interaction between **1** and CYP1A1, 1A2, 2C8, 2C9, 2C19, 2D6, 2E1, 3A4, and 3A5 is 8.51, 8.70, 31.2, 25.3, 17.1, 20.5, 5.21, 41.4, and 62.9 dimensionless, respectively. Thus, the isoforms 3A4 and 3A5 are the main targets of the assayed compound, agreeing with the experimental data.

Table 1. Normalized depletion velocity for $[Ru_3O(CH_3COO)_5(py)_2(dppzCl)]$ observed during the interaction with rCYP450 and remaining activity in the presence of Tween 80®

Isoform	v[a] / (mol min^{-1} mol^{-1})	RA / %
CYP1A1	0.085	24 ± 1
CYP1A2	0.068	90.9 ± 0.5
CYP2B6	0.090	20 ± 2
CYP2C8	0.046	–
CYP2C9	0.058	96 ± 2
CYP2C19	0.049	65 ± 3
CYP2D6	0.083	101 ± 3
CYP2E1	0.047	19 ± 3
CYP3A4	0.066	18 ± 1
CYP3A5	0.111	107 ± 1

[a]Depletion velocity expressed as mol of compound **1** metabolized over time normalized by the molar content of the isoform. RA: remaining activity.

For CYP3A4 and CYP3A5, **1** interacts with the endogenous heme group (Figures 3a and 3b). From the electrostatic potential map of protein (Figures 3c and 3d), it can be noticed that the heme group is in an electrostatic positive density cavity. At the same time, compound **1** fits nicely in an electrostatic negative density region of the continuity of the same cavity. In this case, the dppzCl phenazine prefers to interact with the amino acid residues than with the heme group. Additionally, molecular docking results suggested hydrophobic, π-stacking, and hydrogen bonds as the main intermolecular forces responsible for the interactive profile of 3A4/3A5 with **1** (Table 2 and Figures 3e and 3f).

Conclusions

For the first time, we reported the interaction of a triruthenium *ortho*-metallated phenazine complex with human CYP450 enzymes. This interaction was verified by the ability of CYP450 enzymes to metabolize the compound $[Ru_3O(CH_3COO)_5(py)_2(dppzCl)]PF_6$ *in vitro*. Taking into account the docking and phenotyping

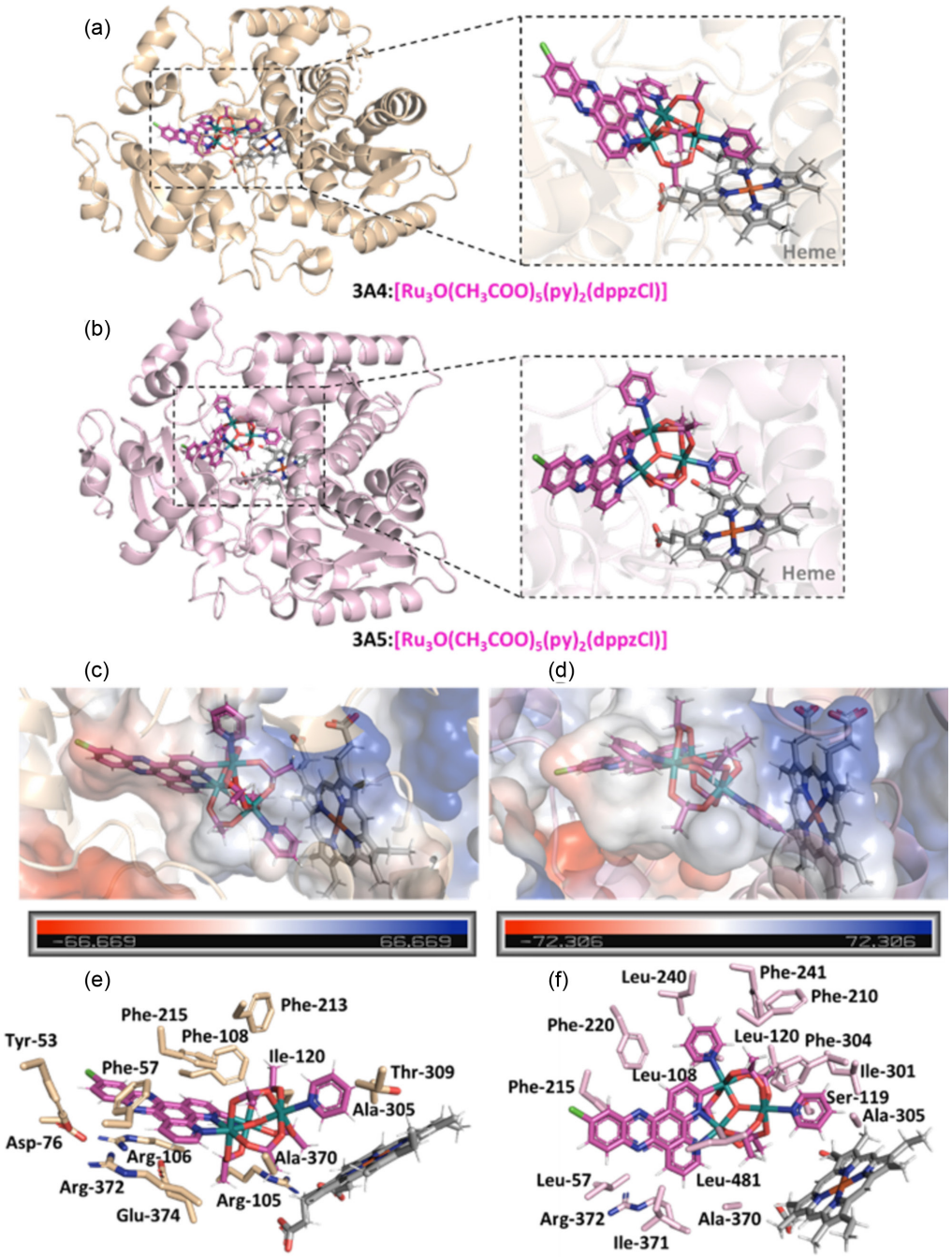

Figure 3. Best docking pose for the interaction (a) 3A4:[$Ru_3O(CH_3COO)_5(py)_2(dppzCl)$] and (b) 3A5:[$Ru_3O(CH_3COO)_5(py)_2(dppzCl)$])] with the corresponding zoom highlighting the interaction between compound **1** and the endogenous heme group. Electrostatic potential map for the interaction (c) 3A4:[$Ru_3O(CH_3COO)_5(py)_2(dppzCl)$] and (d) 3A5:[$Ru_3O(CH_3COO)_5(py)_2(dppzCl)$] with the (e, f) corresponding interactive profile in the presence of the key amino acid residues. Amino acid residues from 3A4 or 3A5, heme, and [$Ru_3O(CH_3COO)_5(py)_2(dppzCl)$] are as stick representation in orange, beige, gray, and pink, respectively. Elements' color: hydrogen, oxygen, chloro, nitrogen, and Ru^{3+} are in white, red, green, dark blue, and dark green, respectively.

results, our study suggests that the isoforms CYP3A4 and CYP3A5 interact preferentially with compound **1**. However, as described previously, the results of phenotyping using supersomes should be interpreted cautiously, considering the inhibitory effect of the surfactant employed. Molecular docking results also helped to identify hydrophobic, π-stacking, and hydrogen bonding as the main intermolecular forces responsible for the interaction profile. The results presented here represent one of the first steps towards further studies on the potential metallo-drug candidate [$Ru_3O(CH_3COO)_5(py)_2(dppzCl)$]$PF_6$ because the CYP450 enzymes modulate drug safety by controlling its plasma concentration. In addition, the knowledge about the isoforms involved in its

Table 2. Molecular docking results for the interaction between 3A4:[$Ru_3O(CH_3COO)_5(py)_2(dppzCl)$] and 3A5:[$Ru_3O(CH_3COO)_5(py)_2(dppzCl)$] into the catalytic pocket of each enzyme.

System	Amino acid residue	Interaction	Interatomic distance / Å
3A4A:[$Ru_3O(CH_3COO)_5(py)_2(dppzCl)$]	Tyr-53	hydrophobic	3.88
	Phe-57	hydrophobic	3.56
	Asp-76	hydrophobic	3.76
	Arg-105	hydrophobic	3.62
	Arg-106	hydrophobic	4.29
	Phe-108	π-stacking	3.51
	Ile-120	hydrophobic	3.23
	Phe-213	hydrophobic	3.13
	Phe-215	π-stacking	3.41
	Ala-305	hydrophobic	3.27
	Thr-309	hydrophobic	3.02
	Ala-370	hydrophobic	2.11
	Arg-372	hydrogen bond	3.47
	Glu-374	hydrophobic	2.99
3A5:[$Ru_3O(CH_3COO)_5(py)_2(dppzCl)$]	Leu-57	hydrophobic	2.92
	Leu-108	hydrophobic	3.89
	Ser-119	hydrogen bond	2.50
	Leu-120	hydrophobic	3.11
	Phe-210	hydrophobic	3.55
	Phe-215	π-stacking	4.00
	Phe-220	hydrophobic	3.74
	Leu-240	hydrophobic	3.11
	Phe-241	hydrophobic	3.85
	Ile-301	hydrophobic	3.43
	Phe-304	π-stacking	4.50
	Ala-305	hydrophobic	2.92
	Ala-370	hydrophobic	3.91
	Ile-371	hydrophobic	3.30
	Arg-372	hydrophobic	3.80
	Leu-481	hydrophobic	3.74

metabolism helps prevent and undestand possible drug-drug interactions.

Supplementary Information

Supplementary information (UV-Vis absorption and ^1H NMR data and spectra of [$Ru_3O(CH_3COO)_5(py)_2(dppzCl)$]$PF_6$, chromatographic method determination, and the determination of the solubilizer agent, bioanalytical method validation and the method for the evaluation of Tween 80® inhibition over rCYP450) is available free of charge at http://jbcs.sbq.org.br as PDF file.

Acknowledgments

The authors are grateful to the Conselho Nacional de Desenvolvimento Científico e Tecnológico (CNPq, grant numbers: 305761/2021; 115798/2020-0; 121857/2021-2; 137362/2022-6; 306186/2021-7), to Fundação de Amparo à Pesquisa do Estado de são Paulo (FAPESP, grant numbers 2022/03478-8 and 2021/10098-4) and to Coordenação de Aperfeiçoamento de Pessoal de Nível Superior (CAPES, grant number 001).

Author Contributions

Luis G. A. Nascimento was responsible for investigation, methodology, visualization, writing original draft, review and editing; Maike F. S. Barbetta for investigation, methodology, visualization; Otávio A. Chaves for investigation, software, writing original draft; Anderson R. M. de Oliveira for conceptualization, visualization, funding acquisition, data curation, writing review and editing; Sofia Nikolaou for conceptualization, visualization, funding acquisition, data curation, writing review and editing.

References

1. Thakral, A.; Verma, M.; Thakur, A.; Bharti, R.; Sharma, R.; *Polycyclic Aromat. Compd*. **2024**, *44*, 1697. [Crossref]
2. Che, Y.-X.; Qi, X.-N.; Qu, W.-J.; Shi, B.-B.; Lin, Q.; *J. Heterocycl. Chem*. **2022**, *59*, 969. [Crossref]

3. Miksa, B.; *Helv. Chim. Acta* **2022**, *105*, e202200066. [Crossref]
4. Yan, J.; Liu, W.; Cai, J.; Wang, Y.; D. Li; Hua, H.; Cao, H.; *Mar. Drugs* **2021**, *19*, 610. [Crossref]
5. Huigens, R. W.; Brummel, B. R.; Tenneti, S.; Garrison, A. T.; Xiao, T.; *Molecules* **2022**, *27*, 1112. [Crossref]
6. Serafim, B.; Bernardino, A. R.; Freitas, F.; Torres, C. A. V.; *Molecules* **2023**, *28*, 1368. [Crossref]
7. Pages, B. J.; Ang, D. L.; Wright, E. P.; Aldrich-Wright, J. R.; *Dalton Trans*. **2015**, *44*, 3505. [Crossref]
8. Kabir, E.; Noyon, M. R. O. K.; Hossain, M. A.; *Results Chem*. **2023**, *5*, 100935. [Crossref]
9. Alessio, E.; Messori, L.; *Molecules* **2019**, *24*, 1995. [Crossref]
10. Lee, S. Y.; Kim, C. Y.; Nam, T. G.; *Drug Des., Dev. Ther*. **2020**, *14*, 5375. [Crossref]
11. Aksakal, N. E.; Kazan, H. H.; Eçik, E. T.; Yuksel F.; *New J. Chem*. **2018**, *42*, 17538. [Crossref]
12. Pauwels, B.; Boydens, C.; Daele, L. V.; de Voorde, J. V.; *J. Pharm. Pharmacol*. **2016**, *68*, 293. [Crossref]
13. Sonkar, C.; Sarkar, S.; Mukhopadhyay, S.; *RSC Med. Chem*. **2022**, *13*, 22. [Crossref]
14. Pragti, B. K. K.; Mukhopadhyay, S.; *Coord. Chem. Rev*. **2021**, *448*, 214169. [Crossref]
15. Toma, H. E.; Araki, K.; Alexiou, A. D. P.; Nikolaou, S.; Dovidauskas, S.; *Coord. Chem. Rev*. **2001**, *219*, 187. [Crossref]
16. Nikolaou, S.; do Nascimento, L. G. A.; Alexiou, A. D. P.; *Coord. Chem. Rev*. **2023**, *494*, 215341. [Crossref]
17. Tauchman, J.; Paul, L. E. H.; Furrer, J.; Therrien, B.; Suess-Fink, G.; *Inorg. Chim. Acta* **2014**, *423*, 16. [Crossref]
18. Possato, B.; Chrispim, P. B. H.; Alves, J. Q.; Ramos, L. C. B.; Marques, E.; de Oliveira, A. C.; R. da Silva, S.; Formiga, A. L. B.; Nikolaou, S.; *Polyhedron* **2020**, *176*, 114261. [Crossref]
19. da Silva, C. F. N.; Chrispim, P. B. H.; Possato, B.; Portapilla, G. B.; Rohrabaugh Jr., T. N.; Ramos, L. C. B.; da Silva, R. S.; de Albuquerque, S.; Turro, C.; Nikolaou, S.; *Dalton Trans*. **2020**, *49*, 16440. [Crossref]
20. Possato, B.; Carneiro, Z. A.; de Albuquerque, S.; Nikolaou, S.; *J. Inorg. Biochem*. **2017**, *176*, 156. [Crossref]
21. da Silva, C. F. N.; Possato, B.; Franco, L. P.; Ramos, L. C. B.; Nikolaou, S.; *J. Inorg. Biochem*. **2018**, *186*, 197. [Crossref]
22. Cacita, N.; Possato, B.; da Silva, C. F. N.; Paulo, M.; Formiga, A. L. B.; Bendhack, L. M.; Nikolaou, S.; *Inorg. Chim. Acta* **2015**, *429*, 114. [Crossref]
23. Di Pietro, M. L.; La Ganga, G.; Nastasi, F.; Puntoriero, F.; *Appl. Sci*. **2021**, *11*, 3038. [Crossref]
24. Peng, X.; Liu, X.; Li, J.; Tan, L.; *J. Inorg. Biochem*. **2022**, *237*, 111991. [Crossref]
25. da Silva, C. F. N.; Al-Afyouni, M.; Xue, C.; Ferreira, F. H. C.; Costa, L. A. S.; Turro, C.; Nikolaou, S.; *Dalton Trans*. **2020**, *49*, 1688. [Crossref]
26. Agência Nacional de Vigilância Sanitária (ANVISA); Resolução da Diretoria Colegiada (RDC) No. 27, de 17 de maio de 2012, *Dispõe sobre Os Requisitos Mínimos para a Validação de Métodos Bioanalíticos Empregados em Estudos com Fins de Registro e Pós-Registro de Medicamentos*; Diário Oficial da União (DOU), Brasília, de 22/05/2012. [Link] accessed in July 2024
27. Costa, E. M. A.; Carrão, D. B.; Bucci, J. L. M.; Oliveira, A. R. M.; Machado, T. M.; Ferreira, V. F.; Lima, É. S.; Vasconcellos, M. C.; Magalhães, I. R. S.; *J. Braz. Chem. Soc*. **2022**, *33*, 1145. [Crossref]
28. Rodrigues, A. D.; *Biochem. Pharmacol*. **1999**, *57*, 465. [Crossref]
29. Berman, H. M.; Westbrook, J.; Feng, Z.; Gilliland, G.; Bhat, T. N.; Weissig, H.; Shindyalov, I. N.; Bourne, P. E.; *Nucleic Acids Res.* **2000**, *28*, 235. [Crossref]
30. Walsh, A. A.; Szklarz, G. D.; Scott, E. E.; *J. Biol. Chem*. **2013**, *288*, 12932. [Crossref]
31. Sansen, S.; Yano, J. K.; Reynald, R. L.; Schoch, G. A.; Griffin, K. J.; Stout, C. D.; Johnson, E. F.; *J. Biol. Chem*. **2007**, *282*, 14348. [Crossref]
32. Schoch, G. A.; Yano, J. K.; Wester, M. R.; Griffin, K. J.; Stout, C. D.; Johnson, E. F.; *J. Biol. Chem*. **2004**, *279*, 9497. [Crossref]
33. Wester, M. R.; Yano, J. K.; Schoch, G. A.; Yang, C.; K. Griffin, J.; Stout, C. D.; Johnson, E. F.; *J. Biol. Chem*. **2004**, *279*, 35630. [Crossref]
34. Reynald, R. L.; Sansen, S.; Stout, C. D.; Johnson, E. F.; *J. Biol. Chem*. **2012**, *287*, 44581. [Crossref]
35. Wang, A.; Stout, C. D.; Zhang, Q.; Johnson, E. F.; *J. Biol. Chem*. **2015**, *290*, 5092. [Crossref]
36. Porubsky, P. R.; Meneely, K. M.; Scott, E. E.; *J. Biol. Chem*. **2008**, *283*, 33698. [Crossref]
37. Williams, P. A.; Cosme, J.; Vinković, D. M.; Ward, A.; Angove, H. C.; Day, P. J.; Vonrhein, C.; Tickle, I. J.; Jhoti, H.; *Science* **2004**, *305*, 683. [Crossref]
38. Wang, J.; Buchman, C. D.; Seetharaman, J.; Miller, D. J.; Huber, A. D.; Wu, J.; Chai, S. C.; Garcia-Maldonado, E.; Wright, W. C.; Chenge, J.; Chen, T.; *J. Am. Chem. Soc*. **2021**, *143*, 18467. [Crossref]
39. *Spartan'18*; Wavefunction Inc.; Irvine, CA, USA, 2020.
40. Shao, Y.; Molnar, L. F.; Jung, Y.; Kussmann, J.; Ochsenfeld, C.; Brown, S. T.; Gilbert, A. T. B.; Slipchenko, L. V.; Levchenko, S. V.; O'Neill, D. P.; DiStasio, R. A.; Lochan, R. C.; Wang, T.; Beran, G. J. O.; Besley, N. A.; Herbert, J. M.; Lin, C. Y.; Voorhis, T. V.; Chien, S. H.; Sodt, A.; Steele, R. P.; Rassolov, V. A.; Maslen, P. E.; Korambath, P. P.; Adamson, R. D.; Austin, B.; Baker, J.; Byrd, E. F. C.; Dachsel, H.; Doerksen, R. J.; Dreuw, A.; Dunietz, B. D.; Dutoi, A. D.; Furlani, T. R.; Gwaltney, S. R.; Heyden, A.; Hirata, S.; Hsu, C. P.; Kedziora, G.; Khalliulin, R. Z.; Klunzinger, P.; Lee, A. M.; Lee, M. S.; Liang, W.; Lotan, I.; Nair, N.; Peters, B.; Proynov, E. I.; Pieniazek, P. A.; Rhee,

Y. M.; Ritchie, J.; Rosta, E.; Sherrill, C. D.; Simmonett, A. C.; Subotnik, J. E.; Woodcock, H. L.; Zhang, W.; Bell, A. T.; Chakraborty, A. K.; Chipman, D. M.; Keil, F. J.; Warshel, A.; Hehre, W. J.; Schaefer, H. F.; Kong, J.; Krylov, A. I.; Gill, P. M. W.; Head-Gordon, M.; *Phys. Chem. Chem. Phys*. **2006**, *8*, 3172. [Crossref]

41. *GOLD*, version 2022.3; Cambridge Crystallographic Data Centre; Cambridge, CB2 1EZ, UK, 2022.
42. Hartshorn, M. J.; Verdonk, M. L.; Chessari, G.; Brewerton, S. C.; Mooij, W. T. M.; Mortenson, P. N.; Murray, C. W.; *J. Med. Chem*. **2007**, *50*, 726. [Crossref]
43. Protein-Ligand Interaction Profiler, https://plip-tool.biotec.tu-dresden.de/plip-web/plip/index, accessed in July 2024.
44. Adasme, M. F.; Linnemann, K. L.; Bolz, S. N.; Kaiser, F.; Salentin, S.; Haupt, V. J.; Schroeder, M.; *Nucleic Acids Res*. **2021**, *49*, W530. [Crossref]
45. *PyMOL Molecular Graphics System*, 1.0 level; Delano Scientific LLC software, Schrödinger; New York, NY, USA, 2007.
46. Yuan, S.; Chan, H. C. S.; Hu, Z.; *Wiley Interdiscip. Rev.: Comput. Mol. Sci*. **2017**, *7*, e1298. [Crossref]
47. Zhang, P.; Sadler, P. J.; *Eur. J. Inorg. Chem*. **2017**, *2017*, 1541. [Crossref]
48. Graf, N.; Lippard, S. J.; *Adv. Drug Delivery Rev*. **2012**, *64*, 993. [Crossref]
49. Klaassen, C. D.; Watkins III, J. B.; *Casarett & Doull's: Essentials of Toxicology*, 3rd ed.; McGraw Hill Medical: New York, USA, 2015.
50. Park, E.; Kim, H. K.; Jee, J. H.; Hahn, S.; Jeong, S.; Yoo, J.; *Toxicol. Appl. Pharmacol*. **2019**, *385*, 114790. [Crossref]
51. Seuanes, G. C.; Moreira, M. B.; Petta, T.; del Lama, M. P. F. M.; de Moraes, L. A. B.; de Oliveira, A. R. M.; Naal, R. M. Z. G.; Nikolaou, S.; *J. Inorg. Biochem*. **2015**, *153*, 178. [Crossref]
52. de Oliveira, A. R. M.; da Fonseca, P.; Curti, C.; da Silva, R. S.; Bonato, P. S.; *Nitric Oxide* **2009**, *21*, 14. [Crossref]
53. Randall, K.; Cheng, S. W.; Kotchevar, A. T.; *In Vitro Cell. Dev. Biol.: Anim.* **2011**, *47*, 631. [Crossref]
54. Nagar, S.; Argikar, A. U.; Tweedie, D. J. In *Enzyme Kinetics in Drug Metabolism Fundamentals and Applications*; Springer: Totowa, USA, 2014. [Crossref]
55. Zhang, Z.; Tang, W.; *Acta Pharm. Sin. B* **2018**, *8*, 721. [Crossref]
56. Zanger, U. M.; Schwab, M.; *Pharmacol. Ther*. **2013**, *138*, 103. [Crossref]

Submitted: January 5, 2024
Published online: July 23, 2024